Asian Journal of Chemistry; Vol. 37, No. 6 (2025), 1458-1468

ASIAN JOURNAL OF CHEMISTRY

https://doi.org/10.14233/ajchem.2025.33854

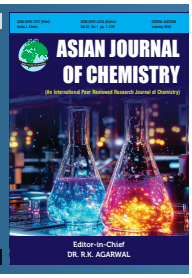

Oxidation of Styrene Catalyzed by Recyclable Polystyrene-Supported Pyrrole-2-Carboxaldehyde Metal Catalysts

SUNIL KUMAR[1], PRAVEEN KUMAR GUPTA[1,*], AMIT KUMAR[2,*] and RAMESH KUMAR[3]

[1]Department of Chemistry, Maharishi Markandeshwar (Deemed to be University), Mullana-133207, India
[2]Department of Chemistry, Indira Gandhi National College, Ladwa, Kurukshetra-136132, India
[3]Department of Chemistry, Kurukshetra University, Kurukshetra-136119, India

*Corresponding authors: E-mail: parveen.gupta@mmumullana.org; amitvash76@gmail.com

Received: 1 April 2025; *Accepted*: 17 May 2025; *Published online*: 27 May 2025; AJC-22019

Polymer-supported heterogeneous catalysts were synthesized by anchoring pyrrole-2-carboxaldehyde on amino-methylated polystyrene and then loading V(IV), Mn(II), Ni(II) and Cu(II) ions on it. The resulting catalysts were characterized by CHNS analysis, FTIR, EDX, DRS, ESR and AAS spectral study confirming the successful immobilization of the metal complexes. The catalytic activity and selectivity of the polymer-supported catalysts were analyzed for the liquid phase oxidation of styrene mediated by H_2O_2 and *tert*-butyl hydroperoxide. The influence of reaction time, temperature and concentration of the catalyst for the oxidation of styrene were examined under optimal conditions (0.1 g catalyst; 6 h reaction time and 60 ºC temperature). A conversion rate of 96.5% was accomplished using a copper catalyst employing H_2O_2 as oxidant, while a selectivity of 90.1% for benzaldehyde formation was reached with a nickel catalyst utilizing *tert*-butyl hydroperoxide (TBHP) as oxidant. The mechanism of the oxidation of styrene in the presence of synthesized catalyst has also been proposed. The catalysts were recovered by simple filtration and reused four times without any significant loss in their activity, proving their truly heterogeneous nature.

Keywords: Polymeric support, Functionalized polymer, Catalyst, Recyclability, Styrene, Oxidation.

INTRODUCTION

The catalysis process plays an indispensable role, enabling the efficient transformation of molecules to create valuable products while minimizing waste and energy consumption [1]. Transition metal complexes have emerged as powerful catalysts in various chemical transformations due to their diverse reactivity and tenable properties [2]. Due to the easy catalyst separation and recyclability the development of supported catalysts has gained significant attention as they combine the advantages of homogeneous catalysis [3]. Polymer-supported catalysts, in particular, have acquired interest within the scientific community owing to their unique ability to immobilize catalytic species on a solid support, offering enhanced stability, insolubility, control of degree of crosslinking, compatibility with most of the solvents and ease of handling and recyclability [4,5]. Among these, amino-methylated transition metal complexes have emerged as a promising class of catalysts, capable of mediating a wide range of reactions with high efficiency and selectivity [6].

The polymer-supported catalysts have special attributes, such as the potential to modify the electronic and steric properties of the metal centre to which they are bound. This results in a catalyst platform that can be tailored to suit specific reaction requirements. Furthermore, the compatibility of such catalyst with polymer matrices provides a robust and versatile platform for immobilizing transition metal complexes [7,8]. The design, synthesis and application of polymer-supported metal complexes along with their catalytic activity have been explored across a broad spectrum of chemical transformations [9-12]. Moreover, authors have explored these catalysts as challenges and prospects, highlighting their potential for sustainable and environmentally friendly chemical processes ultimately contributing to the advancement of catalysis and promoting the development of efficient and sustainable chemical transformations in the modern era [13-16]. Polymer-supported transition metal catal-

ysts derived from functionalized polystyrene resin have been used in various organic reactions, which encouraged to explore the functionalized polystyrene-supported transition metal complexes for the epoxidation of styrene.

Epoxidation of styrene can introduce functional groups into the styrene molecule leading to the formation of new compounds with different chemical properties. Epoxidized styrene derivatives can serve as intermediates in the synthesis of various chemicals and surface modification of materials, which results in improving their adhesion properties and it can be a part of the process to develop functional materials [17-20]. One of the major products obtained in this epoxidation is styrene oxide, whose importance lies in its versatility and applications across different industries. Some key areas highlighting its significance are, as a chemical intermediate, precursor in the production of polystyrene, in the production of resins, a building block for the synthesis of surfactant chemicals and in the biological and medicinal applications [21,22]. The second important product of this epoxidation is benzaldehyde, which has a distinctive almond-like aroma and is widely used in the flavour and fragrance industry, utilized as a flavouring agent in various food products, serves as a building block in the synthesis of pharmaceuticals and as a versatile precursor in organic synthesis [23,24]. The other important products in this epoxidation process include benzoic acid and phenyl ethanol. In this account, V(IV), Mn(II), Ni(II) and Cu(II) ions have been immobilized on pyrrole-2-carboxaldehyde functionalized-amino methylated polystyrene and have been investigated as an effective catalyst activity for the epoxidation of styrene using oxidants like H_2O_2 and *tert*-butyl hydroperoxide.

EXPERIMENTAL

Amino-methylated polystyrene cross-liked with divinylbenzene obtained as a gift from Thermax Chemical Limited Pune, India, pyrrole-2-carboxyaldehyde (Sigma-Aldrich), vanadyl sulphate pentahydrate, nickel acetate tetrahydrate, copper chloride, manganese acetate tetrahydrate, silver nitrate, ammonium thiocyanate, dimethylformamide, conc. nitric acid, hydrogen peroxide (30%), *tert*-butyl hydroperoxide (TBHP) (70%), acetonitrile and methanol (CDH) were used. All the reagents used were of analytical grade and were dried following the standard procedures without further purification.

Characterization: The FT-IR spectra were obtained using a Shimadzu IR Spirit Fourier transform infrared spectrophotometer in the range of 4000-400 cm^{-1}. The reflectance spectra were recorded from UV-2600 Shimadzu doubled beam spectrophotometer using $BaSO_4$ as standard. Energy-dispersive X-ray (EDX) spectra were recorded in FEG scanning electron microscope Hitachi SU8010 Series, CHNS was recorded on Thermo Scientific flash 2000, EPR spectra were recorded on JES-FA200, Metal analysis was done using atomic absorption spectrophotometer (Shimadzu ASC-6880) and GC-MS was recorded in Agilent 7000 GC/TQ.

Acid catalyzed synthesis of polymer-supported ligand: Amino-methylated polystyrene [$PSCH_2$-NH_2] (2 g) was suspended in methanol (20 mL) for 1 h. Pyrrole-2-carboxyaldehyde (0.86 g) dissolved in 15 mL methanolic solution, a small amount of ethanoic acid was added to the suspension to keep the pH of mixture between 3.5 to 4.0. The mixture was refluxed while stirring at 80 ºC for 8 h. During reflux, the colour of the solution becomes yellowish after 1 h and becomes mustard yellow after 3 h. The mixture was cooled, vacuum filtered and washed multiple times with hot methanol, ethanol and acetone and finally dried in air oven at 80 ºC. The same reaction required 48 h to reach completion without the presence of an acid catalyst (**Scheme-I**).

Synthesis of polymer-supported metal catalyst: Polymer-supported ligand [$PSCH_2$-PCA] (4.5 mmol) was allowed to be

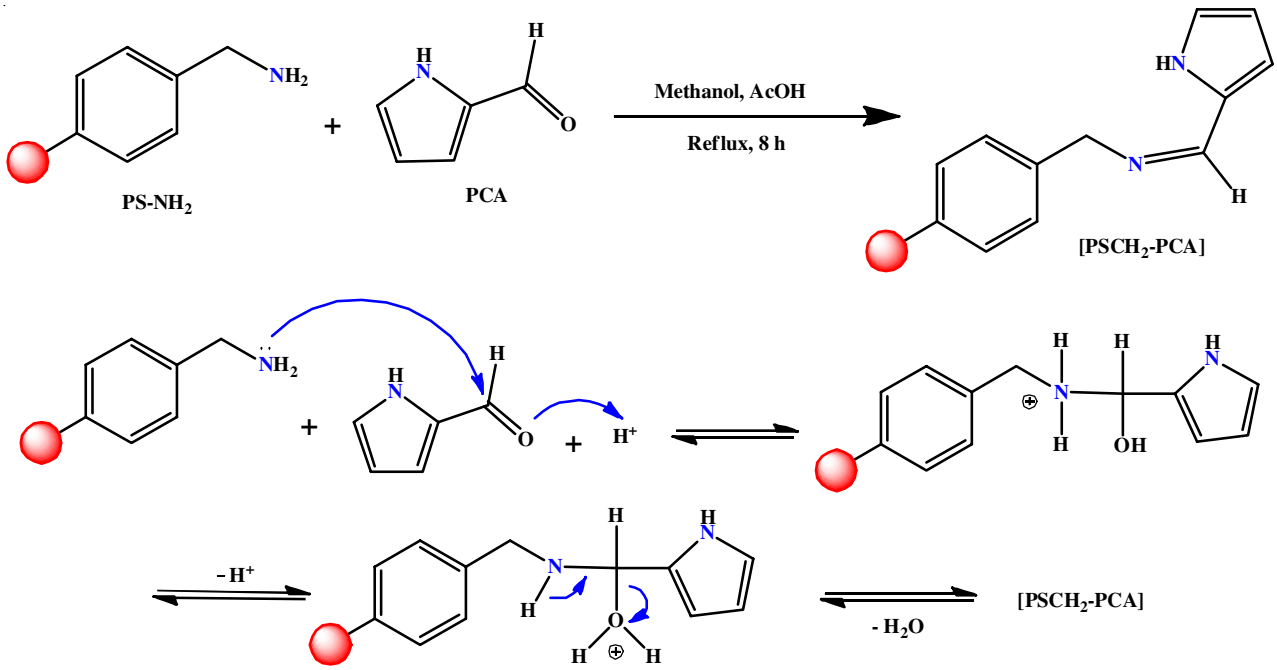

Scheme-I: Synthesis and mechanism of acid catalyzed synthesis of polymer-supported ligand

suspended in methanol (15 mL) for 1 h. $VOSO_4 \cdot 5H_2O/CuCl_2/Mn(CH_3COO)_2 \cdot 4H_2O/NiCl_2 \cdot 6H_2O$ (4.5-9.0 mmol) dissolved in methanol was then added to the above suspension. The colour of the resin starts changing with the progress of the reaction. After refluxing it for 8 h, it was cooled to room temperature, filtered under vacuum and washed repeatedly with hot methanol, ethanol and acetone. It was dried in the oven at 80 ºC (**Scheme-II**).

Catalytic oxidation reaction: The reaction for catalytic oxidation was conducted in a round-bottom flask immersed in a thermostatted oil bath. As per the procedure, the catalyst was pre-soaked in acetonitrile (20 mL) for 30 min. Subsequently, styrene (10 mmol) and the oxidant (10 mmol) were added, followed by the catalyst (0.05-1.0 g). The progress of the reaction was monitored using thin-layer chromatography (TLC). Various reaction conditions were explored, including different catalyst

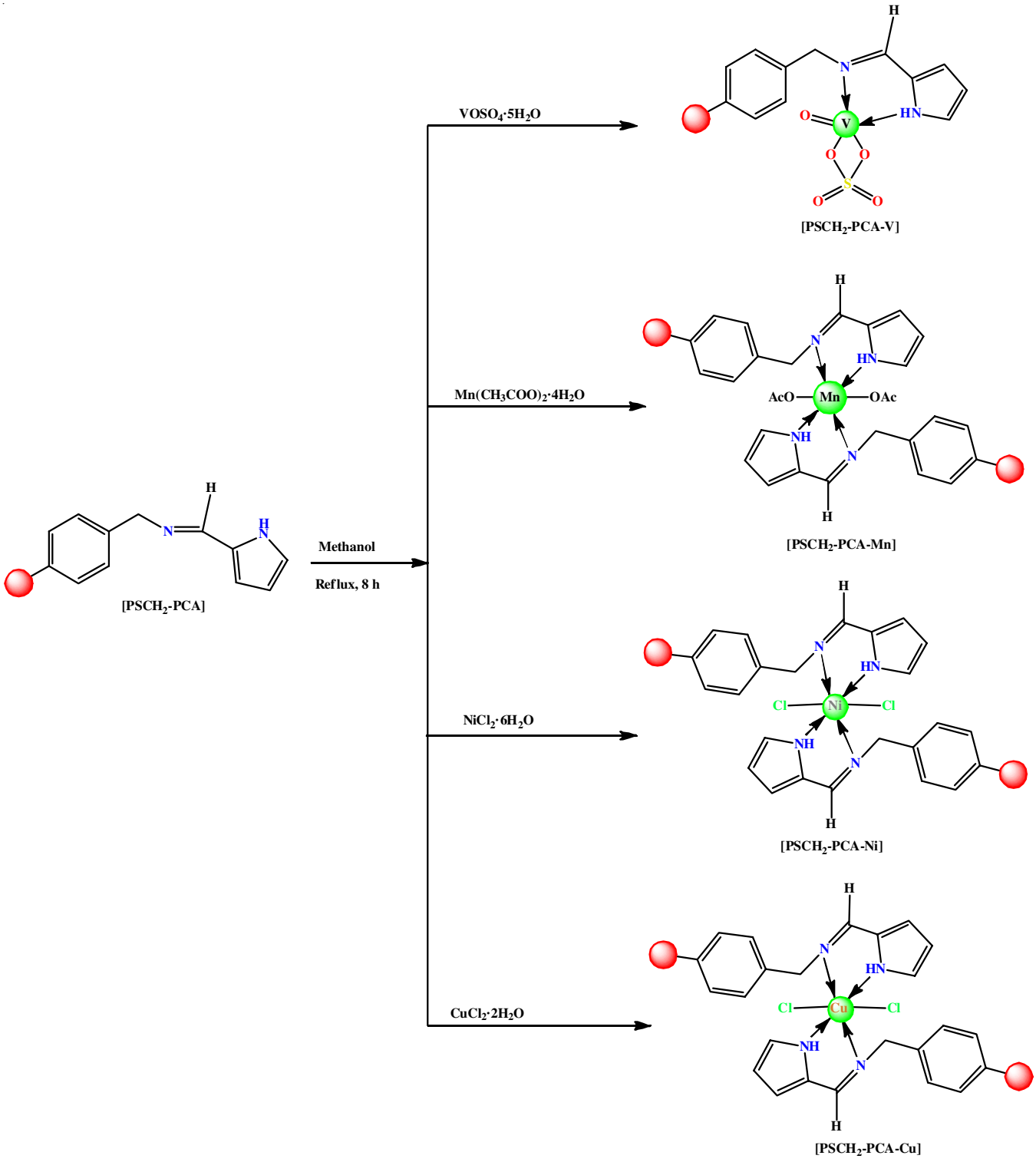

Scheme-II: Synthesis of polymer-supported metal catalysts

amounts (0.05-0.1 g), types of oxidants (TBHP, H_2O_2), reaction temperatures and reaction times (4-8 h). The catalyst was separated by filtration upon reaction completion and the product formation was confirmed using GC-MS analysis.

RESULTS AND DISCUSSION

The cross-linked aminomethylated polystyrene was functionalized with pyrrole-2-carboxaldehyde in the presence of a few drops of ethanoic as catalyst, which leads to the formation of polymer-supported ligand [PSCH$_2$-PCA] (**Scheme-I**). The attachment of ligand with the polymer was primarily confirmed by the ninhydrin test. It is important to mention that the same reaction took 48 h to complete in the absence of an acid catalyst. The polymer functionalized with ligands at the *para* position of phenyl ring of its backbone is depicted in Fig. 1. The binding of the metal salts with functionalized beads to form polymer-supported metal catalysts (**Scheme-II**) was initially indicated by the colour change of the beads.

The analytical data for the polymer-supported ligand and its metal catalysts, derived from CHNS and AAS analyses, are shown in Table-1. From these data, the amount of ligand and metal incorporated in amino-methylated polystyrene was determined which suggests the ligand to metal stoichiometry.

The loading of the ligand and the incorporation of the metal ion into the polymer support were also confirmed through EDX analysis (Fig. 2). [PSCH$_2$-PCA] exhibits only C and N signals, confirming the anchoring of ligand to the polymer. The presence of metal ion signals in all catalysts indicates the binding of the respective metal ions to [PSCH$_2$-PCA]. In the EDX spectra of copper and nickel catalysts, a Cl signal is observed, while the vanadium catalyst shows an S signal, suggesting the coordination of Cl and S atoms, respectively.

FT-IR spectral studies: The overley spectra of the compounds are shown in Fig. 3. The significant IR bands of the polymer-supported pyrrole-2-carboxaldehyde [PSCH$_2$-PCA] and its metal catalysts are shown in Table-2. The spectrum of pyrrole-2-carboxaldehyde (PCA) showed a broad absorption band at 1651 cm^{-1} and 1722 cm^{-1} due to ν(C=C) and ν(C=O), respectively. Comparatively, in [PSCH$_2$-PCA], a new absorption band at 1652 cm^{-1} may be ascribed to ν(C=N) stretching suggests the formation of azomethine functionality. The comp-

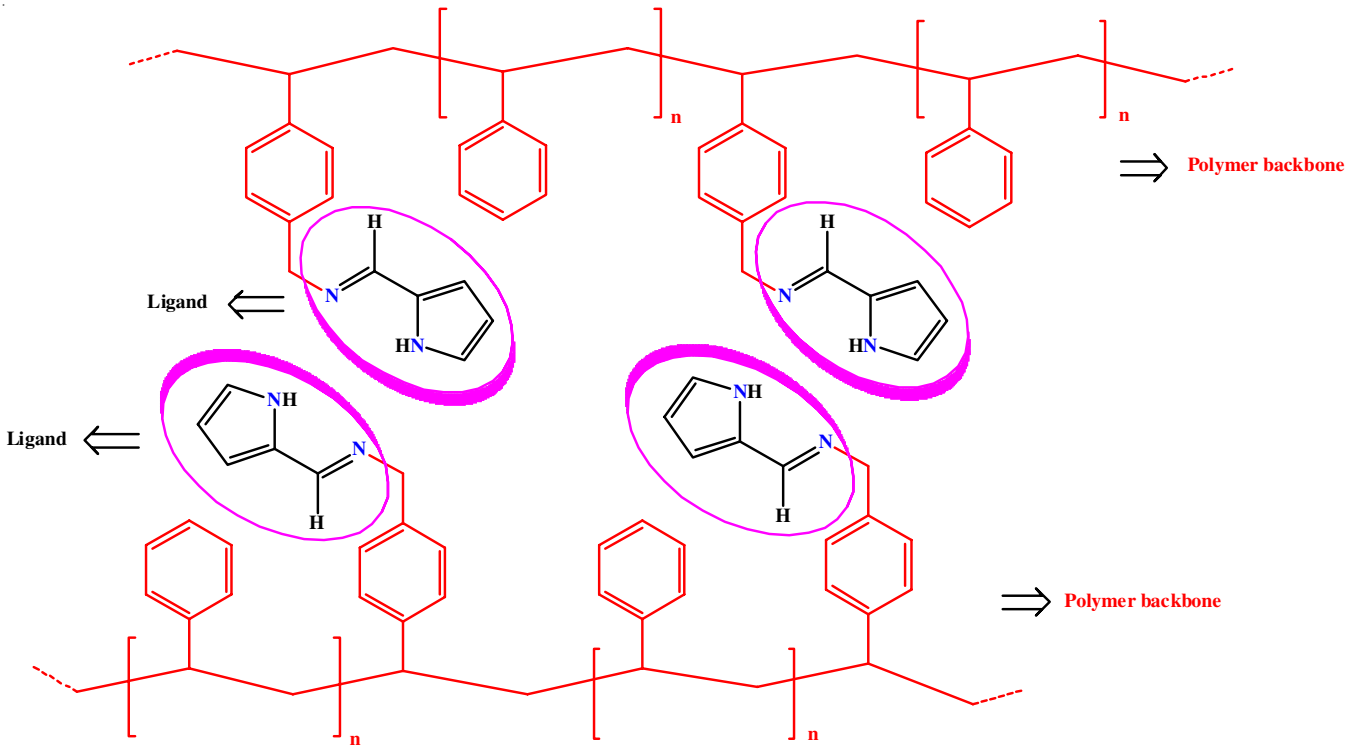

Fig. 1. Functionalized amino-methylated polystyrene beads (neglecting the cross-linking with divinylbenzene)

TABLE-1
ANALYTICAL RESULTS FOR PSCH$_2$-PCA AND ITS METAL CATALYST

Compound	Colour	Elemental analysis (%)					Incorporation (mmol/g of resin)		Ligand:Metal ratio
		C	H	N	S	M	Ligand	Metal	
[PSCH$_2$-PCA]	Light brown	85.1	8.1	6.6	–	–	2.4	–	–
[PSCH$_2$-PCA-V]	Greenish yellow	68.7	6.1	4.7	4.1	6.7	1.68	1.31	1.3:1
[PSCH$_2$-PCA-Mn]	Yellow	76.9	7.0	6.0	–	4.9	2.14	0.89	2.4:1
[PSCH$_2$-PCA-Ni]	Dijon yellow	77.0	7.1	6.2	–	5.6	2.21	0.95	2.2:1
[PSCH$_2$-PCA-Cu]	Light brown	77.3	7.3	5.7	–	5.6	2.04	0.88	2.3:1

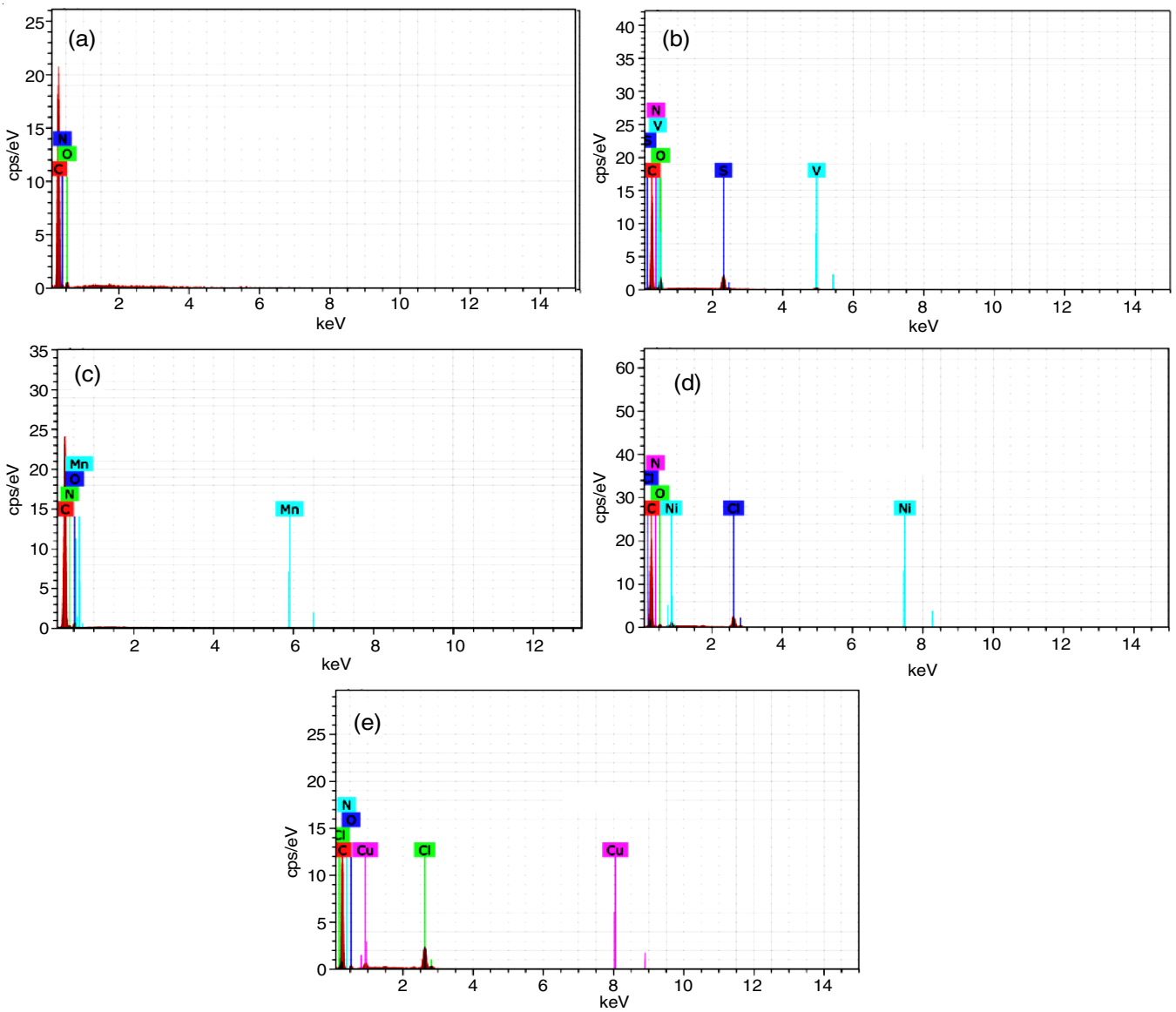

Fig. 2. EDX plot of (a) [PSCH$_2$-PCA]; (b) [PSCH$_2$-PCA-V]; (c) [PSCH$_2$-PCA-Mn]; (d) [PSCH$_2$-PCA-Ni]; (e) [PSCH$_2$-PCA-Cu]

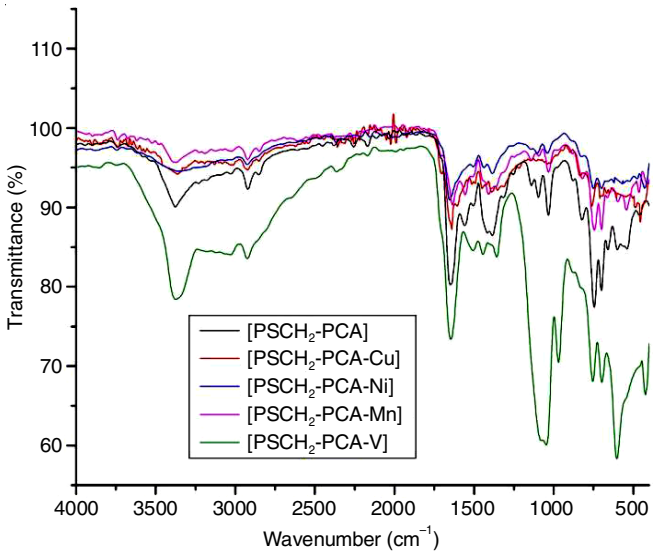

Fig. 3. Overley FT-IR spectra of functionalized polymer and polymer-supported metal catalysts

arison of the infrared spectra of [PSCH$_2$-PCA] and its metal catalysts demonstrated that the ligand bonds to metal ions in a bidentate mode. The band due to ν(C=N) shifts to lower frequencies, appearing in the range of 1645-1629 cm^{-1} in various metal catalysts, which indicates coordination of the azomethine nitrogen to the metal ions. A considerable shift in the N–H stretching frequency at 3380 cm^{-1} in [PSCH$_2$-PCA] was observed in all the catalysts, suggesting the involvement of the N–H group [25]. Binding of metal ion with [PSCH$_2$-PCA] is further confirmed by the presence of M-N, M-O and M-Cl bands in the 453-424, 597-539 and 353-359 cm^{-1} regions, respectively. [PSCH$_2$-PCA-Mn] exhibits band in the regions at 1558 cm^{-1} and 1406 cm^{-1} corresponding to ν_{as}(OAc) and ν_s(OAc) stretch respectively, which are in agreement with the acetate groups being monodentate and indicating the covalent nature of metal-oxygen bond. In [PSCH$_2$-PCA-V], a band at 974 cm^{-1} confirms the presence of ν(V=O) stretch. A band observed in the 1105-1025 cm^{-1} region may be assigned to bidentate sulphate [ν_{as}(SO$_4$) and ν_s(SO$_4$)] coordination [26].

TABLE-2
FTIR DATA FOR THE $PSCH_2$-PCA AND ITS COMPLEXES

Polymer-supported compounds	ν(C=N)	ν(N-H)	ν_{sy}(OAc)/ ν_{asy}(OAc)	$\nu_{sy}(SO_4)$/ $\nu_{asy}(SO_4)$	ν(V=O)	ν(M-N)	ν(M-O)	ν(M-Cl)
[$PSCH_2$-PCA]	1652	3380	–	–	–	–	–	–
[$PSCH_2$-PCA-V]	1640	3362		1105, 1025	974	427	597	–
[$PSCH_2$-PCA-Mn]	1629	3369	1558, 1406			453	539	
[$PSCH_2$-PCA-Ni]	1645	3368				424	–	353
[$PSCH_2$-PCA-Cu]	1641	3362				450	–	359

Diffused reflectance spectra: The overlap reflectance spectra of polymer-supported metal catalysts are shown in Fig. 4. The reflectance spectra are very helpful to investigate the structure of solid insoluble compounds (Table-3). The reflectance spectrum of [$PSCH_2$-PCA] shows intra-ligand absorption maxima corresponding to φ→φ*, π→π* and n→π* transitions at 4854, 3460 and 2865 cm^{-1}, respectively which get shifted after complexation. The reflectance spectrum of the vanadium catalyst exhibits three distinct transitions in the region of 12626, 16103 and 24154 cm^{-1}. These transitions fall within the range reported for five coordinated (C_{4v} symmetry) oxovanadium(IV) compounds [27]. These transitions can be assigned to $^2B_2 \rightarrow {}^2E$ ($d_{xy} \rightarrow d_{xz;yz}$), $^2B_2 \rightarrow {}^2B_1$ ($d_{xy} \rightarrow d_{x^2-y^2}$) and $^2B_2 \rightarrow {}^2A_1$ ($d_{xy} \rightarrow d_{z^2}$) in increasing energy. Manganese catalyst shows two weak bands due to $^6A_{1g} \rightarrow {}^4T_{1g}$(G) and $^6A_{1g} \rightarrow {}^4T_{2g}$(G) at 16207 and 20367 cm^{-1}, which suggests its octahedral geometry [28]. Three spin-allowed bands at 9940, 15699 and 24155 cm^{-1} are observed in the electronic spectrum of the nickel(II) catalyst. These bands may be attributed to the $^3A_{2g} \rightarrow {}^3T_{2g}$(G) ($\nu_1$), $^3A_{2g} \rightarrow {}^3T_{1g}$(F) ($\nu_2$) and $^3A_{2g} \rightarrow {}^3T_{1g}$(P) ($\nu_3$) transitions, respectively, confirming the presence of Ni(II) d^8 ions in an octahedral coordination environment [28]. The octahedral geometry was further supported by ν_2:ν_1 ratio (1.6) found for the usual octahedral nickel compounds. The reflectance spectra of copper catalyst exhibit $d \rightarrow d$ bands at 10870; 12151 and 20366 cm^{-1}, attributed to $^2B_{1g} \rightarrow {}^2A_{1g}$ ($d_{x^2-y^2} \rightarrow d_{z^2}$); $^2B_{1g} \rightarrow {}^2B_{2g}$ ($d_{x^2-y^2} \rightarrow d_{xy}$); $^2B_{1g} \rightarrow {}^2E_g$ ($d_{x^2-y^2} \rightarrow d_{xz,yz}$) transitions, respectively, due to the distorted octahedral geometry (D_{4h}) [28].

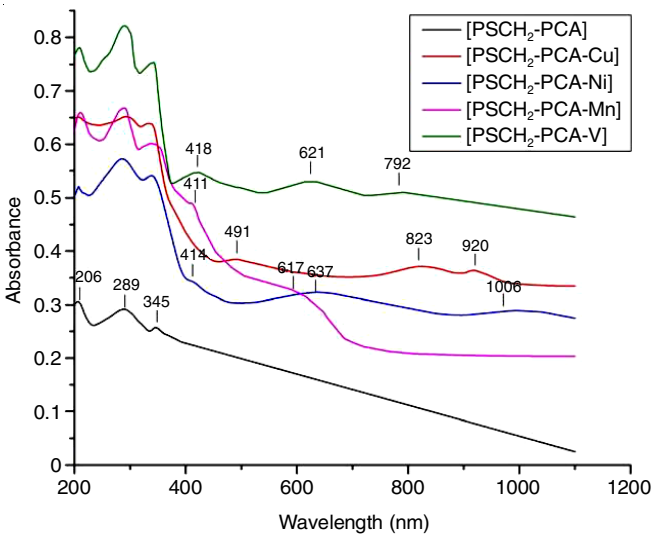

Fig. 4. Overlap DRS spectra of polymer-supported metal catalysts

EPR study: The EPR spectra of vanadium, manganese and copper catalysts were obtained at room temperature and are presented in Fig. 5. The vanadium catalyst displays an axially symmetrical signal typical of the V(IV) ion. The eight well-resolved lines [^{51}V; I = 7/2; 2nI + 1 = 8) appear in both parallel and perpendicular regions attributed to the coupling of an unpaired electron of V(IV) to its own nuclear spin. The well-resolved hyperfine lines suggest that the V^{4+} ions are uniformly dispersed within the polymeric support, with negligible vanadium-vanadium interactions. The spectrum is anisotropic with Hamiltonian parameters: $g_\perp > g_\parallel$ ($g_\perp$ = 2.0 and $g_\parallel$ = 1.90) and $A_\perp > A_\parallel$ ($A_\perp$ = 193 G and $A_\parallel$ = 77 G). The values represent square pyramidal complexes with V=O bond along the *z*-axis with C_{4v} symmetry [29]. EPR of the Mn(II) complex (Fig. 5b) shows six hyperfine lines, arising from the interaction of the electron spin with the nuclear spin (^{55}Mn, I = 5/2, 2nI + 1 = 6). The A values are also consistent with an octahedral coordination. The Hamiltonian parameters obtained from the analyses of the spectra were A = 90.3 G and g = 1.997, which are characteristic of Mn(II) complexes with axial symmetry and octahedral geometry [30]. Copper catalyst exhibits a typical axial spectrum with $g_\parallel > g_\perp > g_e$ ($g_\parallel$ = 2.27 and $g_\perp$ = 2.07), revealing hyperfine splitting in the parallel region (^{55}Cu, I = 3/2, 2nI + 1 = 4) (Fig. 5c). The hyperfine lines split the $g_\parallel$ signals with an average spacing of 133 G, indicating the uniform distribution of Cu(II) complexes within the polymer matrix and the absence of Cu–Cu interactions. However, the perpendicular region of the spectrum is less resolved. On the other hand, the perpendicular region of the spectra is not well resolved. The g value indicates that the unpaired electron of copper resides in $d_{x^2-y^2}$ in orbital [30].

Catalytic activity: The effectiveness of the synthesized catalysts was evaluated through oxidation reactions of styrene. Polymer-anchored V(IV), Mn(II), Ni(II) and Cu(II) catalysts

TABLE-3
REFLECTANCE SPECTRAL DATA OF POLYMER SUPPORTED METAL COMPLEXES

Polymer-supported metal catalysts	*d-d* Band position (cm^{-1})	*d-d* Band assignment
[$PSCH_2$-PCA-V]	12626, 16103, 24154	$^2B_2 \rightarrow {}^2E$, $^2B_2 \rightarrow {}^2B_1$, $^2B_2 \rightarrow {}^2A_1$
[$PSCH_2$-PCA-Mn]	16207, 20367	$^6A_{1g} \rightarrow {}^4T_{1g}$(G), $^6A_{1g} \rightarrow {}^4T_{2g}$(G)
[$PSCH_2$-PCA-Ni]	9940, 15699, 24155	$^3A_{2g} \rightarrow {}^3T_{2g}$(G) ($\nu_1$), $^3A_{2g} \rightarrow {}^3T_{1g}$(F) ($\nu_2$), $^3A_{2g} \rightarrow {}^3T_{1g}$(P) ($\nu_3$)
[$PSCH_2$-PCA-Cu]	10870, 12151, 20366	$^2B_{1g} \rightarrow {}^2A_{1g}$, $^2B_{1g} \rightarrow {}^2B_{2g}$, $^2B_{1g} \rightarrow {}^2E_g$

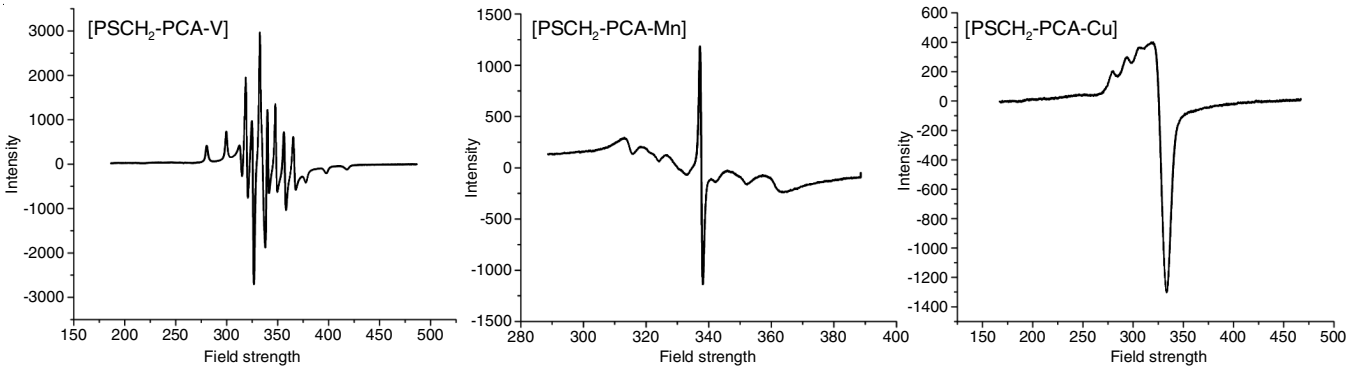

Fig. 5. EPR plot of [$PSCH_2$-PCA-V], [$PSCH_2$-PCA-Mn] and [$PSCH_2$-PCA-Cu]

were employed in these reactions. The reaction yielded benzaldehyde, styrene oxide and benzoic acid as primary products, along with minor quantities of unidentified byproducts. We systematically investigated the influence of oxidants, reaction time, reaction temperature and catalyst dosage on product yield. This comprehensive study aimed to optimize reaction conditions and enhance the overall efficiency of the oxidation process.

Effect of oxidant: To optimize catalytic performance, we investigated the effectiveness of TBHP and H_2O_2 for styrene oxidation. Without an oxidant, the reaction failed to proceed. According to Tables 4 and 5, TBHP in an acetonitrile medium proved to be the most efficient oxidant for styrene oxidation, possibly due to TBHP's inertness without a catalyst and its solubility in acetonitrile. Conversely, H_2O_2 exhibited higher efficiency than TBHP for the styrene conversion.

TABLE-4
CONVERSION OF STYRENE AND PRODUCT SELECTIVITY

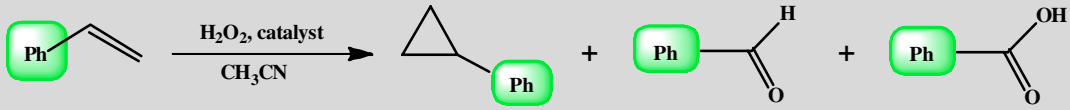

Catalyst	Amount of catalyst (g)	Time (h)	% Conversion#	% Selectivity#			
				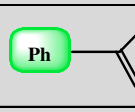	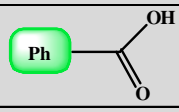	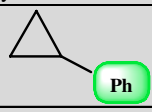	Others
Blank test		4	6.5	84.4	5.9	3.7	6.0
		5	9.7	85.2	5.8	3.6	5.4
		6	9.8	88.6	6.9	2.1	2.4
[$PSCH_2$-PCA-V]	0.05	4	59.1	70.5	10.4	2.5	16.6
		5	79.2	77.8	9.6	9.8	2.8
		6	88.5	76.7	10.4	10.2	2.7
	0.1	4	61.2	75.4	11.0	8.8	4.8
		5	84.1	77.2	10.4	7.9	4.5
		6	93.2	76.5	10.4	10.0	3.1
[$PSCH_2$-PCA-Mn]	0.05	4	48.8	80.8	10.6	5.0	3.6
		5	72.2	82.4	10.0	6.4	1.2
		6	78.0	82.4	10.1	5.8	1.7
	0.1	4	66.8	82.2	8.5	4.9	4.4
		5	79.9	82.0	8.9	5.0	4.1
		6	86.1	82.4	10.2	5.8	1.6
[$PSCH_2$-PCA-Ni]	0.05	4	45.0	70.8	7.5	13.0	8.7
		5	66.0	77.8	7.9	12.2	2.1
		6	70.0	78.0	7.5	13.2	1.3
	0.1	4	56.2	78.0	7.5	13.1	1.4
		5	73.8	78.0	7.5	13.1	1.4
		6	76.4	78.2	7.5	13.1	1.2
[$PSCH_2$-PCA-Cu]	0.05	4	55.0	70.5	18.0	8.5	3.0
		5	76.2	68.9	18.0	8.5	4.6
		6	85.0	70.0	18.0	8.5	3.5
	0.1	4	70.2	70.0	17.0	9.2	3.8
		5	90.2	70.4	18.0	7.9	3.7
		6	96.5	70.2	18.0	8.5	3.1

*Conditions: 20 mL CH_3CN, 10 mmol styrene, 10 mmol H_2O_2, 60 ºC; #GC-MS.

TABLE-5
CONVERSION OF STYRENE AND PRODUCT SELECTIVITY

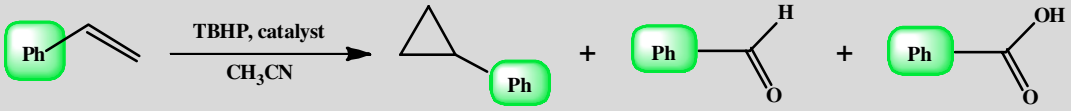

Catalyst	Amount of catalyst (g)	Time (h)	% Conversion#	% Selectivity#			
				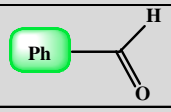	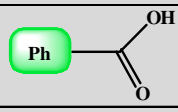	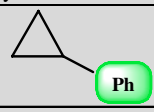	Others
Blank test		4	5.8	80.6	9.0	4.2	6.2
		5	7.2	82.6	9.0	2.0	6.4
		6	10.5	85.6	9.9	2.1	2.4
[PSCH$_2$-PCA-V]	0.05	4	55.7	70.5	5.0	20.1	4.4
		5	68.8	73.4	6.8	19.0.	0.8
		6	83.2	71.5	5.9	20.8	1.8
	0.1	4	47.8	69.0	7.0	22.6	1.4
		5	70.5	71.2	5.8	20.2	4.8
		6	88.7	72.0	5.9	20.6	1.5
[PSCH$_2$-PCA-Mn]	0.05	4	48.9	80.5	5.0	18.0	1.0
		5	66.8	81.2	3.8	12.9	2.1
		6	72.2	81.5	5.7	12.4	2.4
	0.1	4	56.9	81.0	5.8	12.8	0.4
		5	76.9	83.5	4.0	10.2	2.3
		6	85.6	81.5	5.7	10.5	2.3
[PSCH$_2$-PCA-Ni]	0.05	4	68.8	85.8	2.0	7.8	4.4
		5	79.1	88.8	2.0	5.2	4.0
		6	85.5	90.0	2.2	6.1	1.7
	0.1	4	67.8	89.2	1.8	7.2	1.8
		5	85.2	91.5	2.1	4.4	2.0
		6	93.2	90.1	2.3	6.1	1.5
[PSCH$_2$-PCA-Cu]	0.05	4	48.4	65.0	20.0	12.8	2.2
		5	63.3	65.8	17.2	14.8	2.2
		6	75.4	67.0	18.0	13.8	1.2
	0.1	4	52.7	67.0	18.0	13.8	1.2
		5	75.1	67.5	18.0	12.5	2.0
		6	90.8	67.5	18.2	13.4	0.9

*Conditions: 20 mL CH_3CN, 10 mmol styrene, 10 mmol TBHP, 60 ºC; #GC-MS.

Effect of reaction temperature: The impact of reaction temperature on the progress of styrene oxidation employing the synthesized catalysts were studied. Oxidation reactions were conducted with varying temperatures ranging from 40 ºC to 80 ºC, employing a 1:1 mmol ratio of styrene to TBHP or H_2O_2 in an acetonitrile medium for 8 h and the results are summarized in Tables 4 and 5. As expected, styrene conversion increased with rising reaction temperature, however, no conversion was observed at temperatures below 40 ºC. The optimal temperature for the epoxidation process was found to be 60 ºC.

Effect of reaction time: The reaction progress was monitored by conducting styrene reactions with TBHP and H_2O_2 in a 1:1 ratio, using catalyst amounts of 0.05 g and 0.1 g at 60 ºC with continuous stirring. A negligible reaction occurs during the initial 2 h, indicative of an induction period. Subsequently, styrene conversion steadily increased with prolonged reaction times for all catalysts. Comparison of results between 3 to 8 h, as depicted in Fig. 6, demonstrated that the highest styrene conversion rate was achieved after 6 h. Also, the selectivity for different products remained largely unchanged with increasing reaction time.

Effect of amount of catalyst: The influence of catalyst amount on the oxidation of styrene was studied for 0.05 g and 0.1 g catalyst, keeping the styrene/TBHP/and H_2O_2 conc. 10 mmol, temperature 60 ºC and time 6 h. Tables 4 and 5 demonstrate how varying the catalyst amount influences the oxidation of styrene over time. Furthermore, an experiment was conducted using styrene in the presence of TBHP and H_2O_2 but without adding a catalyst. It was observed that in the absence of any added catalyst, the conversion of styrene ranges from 5.8% to 10.5%. At a low catalyst concentration of 0.05 g, moderate conversion of styrene was achieved. Increasing the catalyst amount from 0.05 g to 0.1 g resulted in higher conversion rates of styrene. This could be attributed to the increased availability of active sites on the catalyst, facilitating greater accessibility of substrate and oxidant molecules to the catalyst. Further increases in catalyst amount did not significantly affect styrene conversion, which remained nearly constant.

Catalyst reusability: To assess the reusability of the polymer-anchored metal catalysts, recycling experiments were conducted for the oxidation of styrene. After each experiment, the catalyst was separated *via* simple filtration, washed, dried

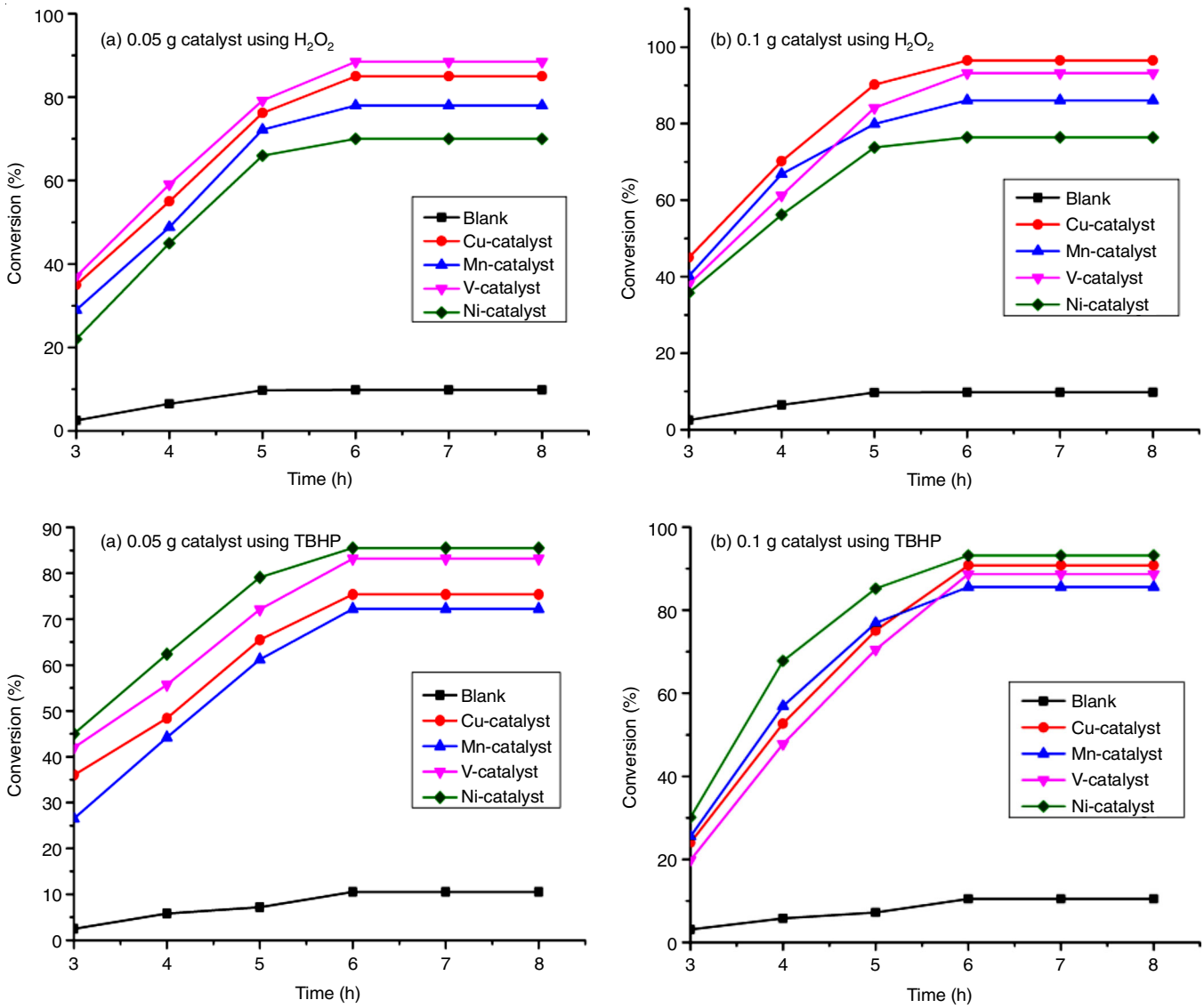

Fig. 6. Effect of percentage conversion of styrene with time at different amounts of catalyst

under vacuum and then used for the next run under identical reaction conditions. The catalytic process was repeated with additional substrate added in appropriate amounts under optimal conditions and the nature and yield of the final product were comparable to those of the initial run. It is evident that after four cycles, there was a slight decrease in conversion, while the product selectivity remained consistent (Fig. 7). The recovered catalyst was analyzed using IR and DRS spectra, which indicated no changes even after multiple reuses. After the separation of the catalyst by filtration, the metal content was also determined by AAS. At the end of the fourth recycle, there was slight loss in the metal content was observed. Based on these findings, it is concluded that these catalysts remain unchanged after their use in the reaction.

Plausible mechanism: Scheme-III shows the probable mechanism for the oxidation of styrene mediated by peroxide (H_2O_2/TBHP) and catalyzed with polymer-supported metal catalyst. Firstly, the metal catalyst interacts with the peroxide to generate hydroperoxyl intermediate (**I**), which looses *tert*-

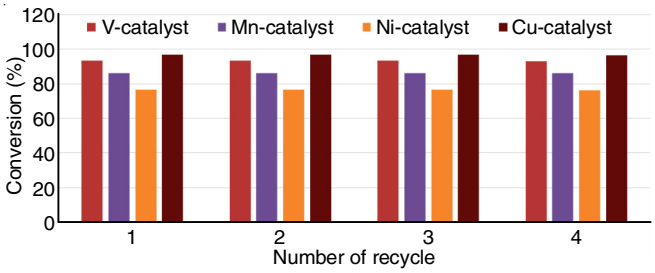

Fig. 7. Recyclability test of polymer-supported metal catalyst

BuOH/H_2O molecule to give metal-oxyl species (**II**). Intermediate **II** interacts with the pi-bond of the styrene to generate styrene oxide. In the next step, the carbon-carbon bond of the styrene oxide gets broken to generate the benzaldehyde as a major product.

Conclusion

Polymer supported metal catalysts *viz*. [PSCH$_2$-PCA-V], [PSCH$_2$-PCA-Mn], [PSCH$_2$-PCA-Ni] and [PSCH$_2$-PCA-Cu]

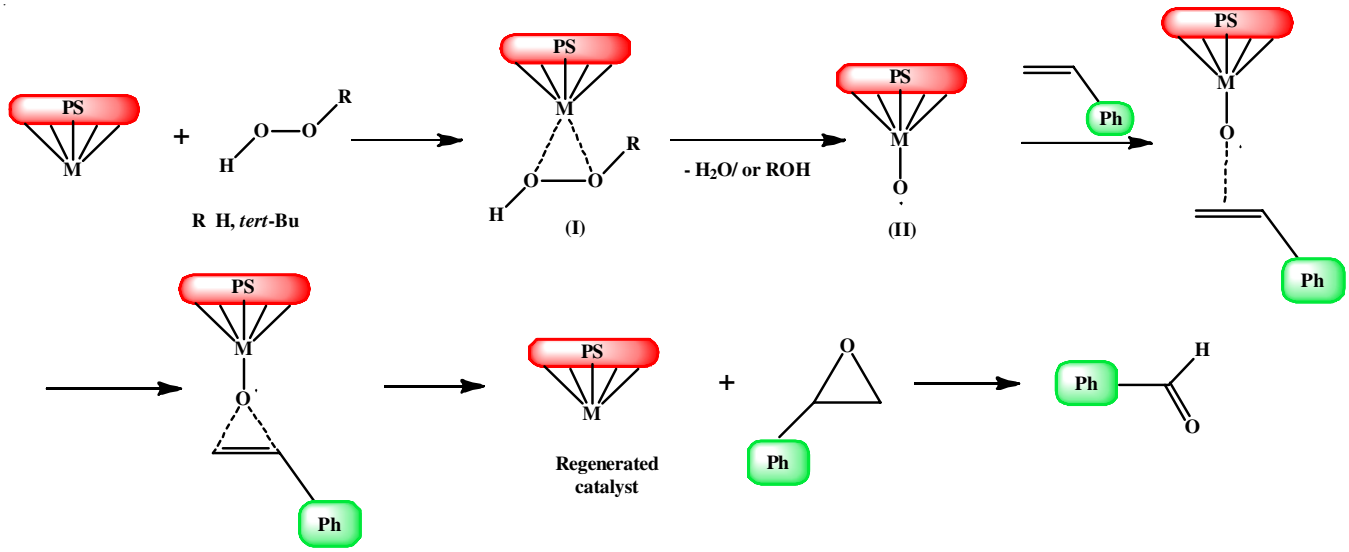

Scheme-III: Proposed mechanism for the H_2O_2/TBHP mediated oxidation of styrene catalyzed by supported metal catalyst

were synthesized by reacting aminomethylated polystyrene and pyrrole-2-carboxaldehyde followed by the reaction of functionalized resin with V(IV), Mn(II), Ni(II) and Cu(II) metal salts. They were analyzed by different analytical and spectroscopic techniques. The potential of the catalysts was investigated for styrene oxidation using 30% H_2O_2 and 70% TBHP. The oxidation of styrene gave three major products namely benzaldehyde, styrene oxide and benzoic acid. Under optimized reaction conditions (0.1 g catalyst concentration, 6 h reaction time and 60 ºC temperature), the percentage conversion of styrene was recorded best for [PSCH$_2$-PCA-Cu] (96.5) and poorest for [PSCH$_2$-PCA-Ni] (76.4) in the presence of H_2O_2 as an oxidizing agent. The percentage selectivity for benzaldehyde formation was highest for [PSCH$_2$-PCA-Ni] (90.1) and lowest for PSCH$_2$-PCA-Cu] (67.5) mediated by TBHP as an oxidant. These catalysts have been successfully reused three times without any loss in their initial activity. All these facts have allowed us to view them as promising heterogeneous catalysts for other transformations that are currently under investigation.

ACKNOWLEDGEMENTS

The authors are thankful to the Maharishi Markandeshwar (Deemed to be University), Mullana, India for providing the research facilities.

CONFLICT OF INTEREST

The authors declare that there is no conflict of interests regarding the publication of this article.

REFERENCES

1. W.N.R.W. Isahak and A. Al-Amiery, *Green Technol. Sustain.*, **2**, 100078 (2024); https://doi.org/10.1016/j.grets.2024.100078
2. J. Takaya, *Chem Sci.*, **12**, 1964 (2020); https://doi.org/10.1039/d0sc04238b
3. J. Lu and P.H. Toy, *Chem. Rev.*, **109**, 815 (2009); https://doi.org/10.1021/cr8004444
4. P.R. Sruthi, R. Roopak and S. Anas, *ChemistrySelect*, **8**, e202204374 (2023); https://doi.org/10.1002/slct.202204374
5. N. Haque, U. Mandi, S.M. Islam and N. Salam, *Prog. Chem. Biol. Sci.*, **72**, 72 (2023); https://doi.org/10.31674/book.2023pcbs008
6. M. Nasrollahzadeh, N. Motahharifar, K. Pakzad, Z. Khorsandi, T. Baran, J. Wang, B. Kruppke and H.A. Khonakdar, *Sci. Rep.*, **13**, 3214 (2023); https://doi.org/10.1038/s41598-023-30198-7
7. M. Sayin, M. Can and M. Imamoglu, *J. Chem. Eng. Data*, **66**, 1132 (2021); https://doi.org/10.1021/acs.jced.0c00920
8. S.M. Lakshminarayana, R. Boregowda and G. Virupaiah, *Chem. Zvesti*, **77**, 3589 (2023); https://doi.org/10.1007/s11696-023-02721-7
9. M.R. Maurya, M. Nandi, A. Patter, F. Avecilla and K. Ghosh, *Catalysts*, **13**, 615 (2023); https://doi.org/10.3390/catal13030615
10. S.M. Islam, P. Mondal, K. Tuhina, A.S. Roy, D. Hossain and S. Mondal, *Transition Met. Chem.*, **35**, 891 (2010); https://doi.org/10.1007/s11243-010-9409-3
11. M.J. Madhura, A.S. Jeevan Chakravarthy, S. Hariprasad and V. Gayathri, *Catal. Lett.*, **153**, 1141 (2023); https://doi.org/10.1007/s10562-022-04055-7
12. C. Yang and L. Cui, *Green Energy Environ.*, **8**, 1 (2023); https://doi.org/10.1016/j.gee.2022.03.004
13. H. Jiang, S. Lu, X. Zhang, H. Peng, W. Dai and J. Qiao, *Catal. Sci. Technol.*, **4**, 2499 (2014); https://doi.org/10.1039/C4CY00436A
14. M.J. Silva, J. Gomes, P. Ferreira and R.C. Martins, *Water*, **14**, 825 (2022); https://doi.org/10.3390/w14050825
15. V.B. Valodkar, G.L. Tembe, M. Ravindranathan and H.S. Rama, *React. Funct. Polym.*, **56**, 1 (2003); https://doi.org/10.1016/S1381-5148(03)00048-8
16. T. Maharana, N. Nath, H.C. Pradhan, S. Mantri, A. Routaray and A.K. Sutar, *React. Funct. Polym.*, **171**, 105142 (2022); https://doi.org/10.1016/j.reactfunctpolym.2021.105142
17. G.N. Wogan, *Semin. Oncol.*, **24**, 227 (1997).
18. Y. Han, L. Wu, Q. Han, R. Zhang and J. Li, *New J. Chem.*, **47**, 3945 (2023); https://doi.org/10.1039/D2NJ05834K
19. Q. Gazu, M. Shozi and P. Mpungose, *MATEC Web Conf., EDP Sciences*, 01004 (2023); https://doi.org/10.1051/matecconf/202337401004
20. W. Zhang, L. Liu, H. Cheng, J. Zhu, X. Li, S. Ye and X. Li, *Mater. Adv.*, **5**, 1364 (2024); https://doi.org/10.1039/D3MA00682D

21. M.A. Andrade and L.M.D.R.S. Martins, *Molecules*, **26**, 1680 (2021); https://doi.org/10.3390/molecules26061680
22. G. Vala, R.N. Jadeja, A. Patel and D. Choquesillo-Lazarte, *Inorg. Chim. Acta*, **563**, 121925 (2024); https://doi.org/10.1016/j.ica.2024.121925
23. W.J. Cui, Q. Zhao, H.T. Zhu, N. Hu, Y.Y. Ma, Z.G. Han and Y.G. Li, *J. Coord. Chem.*, **73**, 2521 (2020); https://doi.org/10.1080/00958972.2020.1821881
24. M. Arian, H. Mollabagher, S. Taheri, A. Zamanian and S.A.H.S. Mousavi, *Turk. J. Chem.*, **45**, 1882 (2021); https://doi.org/10.3906/kim-2101-26
25. M. Shebl, *J. Mol. Struct.*, **1128**, 79 (2017); https://doi.org/10.1016/j.molstruc.2016.08.056
26. V.P. Singh, S. Singh and A. Katiyar, *J. Enzyme Inhib. Med. Chem.*, **24**, 577 (2009); https://doi.org/10.1080/14756360802318662
27. M.K. Sahani, U. Yadava, O.P. Pandey and S.K. Sengupta, *Spectrochim. Acta A Mol. Biomol. Spectrosc.*, **125**, 189 (2014); https://doi.org/10.1016/j.saa.2014.01.041
28. G. Lupascu, E. Pahontu, S. Shova, S.F. Bărbuceanu, M. Badea, C. Paraschivescu, J. Neamtu, M. Dinu, R.V. Ancuceanu, D. Drăgănescu and C.E. Dinu-Pîrvu, *Appl. Organomet. Chem.*, **35**, e6149 (2021); https://doi.org/10.1002/aoc.6149
29. S.M. Islam, A.S. Roy, P. Mondal and N. Salam, *J. Mol. Catal. Chem.*, **358**, 38 (2012); https://doi.org/10.1016/j.molcata.2012.02.009
30. T.H. Bennur, D. Srinivas and P. Ratnasamy, *Micropor. Mesopor. Mater.*, **48**, 111 (2001); https://doi.org/10.1016/S1387-1811(01)00345-6